Pharmaceutical Development and Technology

ISSN: 1083-7450 (Print) 1097-9867 (Online) Journal homepage: https://www.tandfonline.com/loi/iphd20

PHBV/PLGA nanoparticles for enhanced delivery of 5-fluorouracil as promising treatment of colon cancer

Somayeh Handali, Eskandar Moghimipour, Mohsen Rezaei, Zahra Ramezani & Farid Abedin Dorkoosh

To cite this article: Somayeh Handali, Eskandar Moghimipour, Mohsen Rezaei, Zahra Ramezani & Farid Abedin Dorkoosh (2020) PHBV/PLGA nanoparticles for enhanced delivery of 5-fluorouracil as promising treatment of colon cancer, Pharmaceutical Development and Technology, 25:2, 206-218, DOI: 10.1080/10837450.2019.1684945

To link to this article: https://doi.org/10.1080/10837450.2019.1684945

Accepted author version posted online: 25 Oct 2019.
Published online: 20 Nov 2019.

PHARMACEUTICAL DEVELOPMENT AND TECHNOLOGY
2020, VOL. 25, NO. 2, 206–218
https://doi.org/10.1080/10837450.2019.1684945

Taylor & Francis
Taylor & Francis Group

RESEARCH ARTICLE

PHBV/PLGA nanoparticles for enhanced delivery of 5-fluorouracil as promising treatment of colon cancer

Somayeh Handali[a], Eskandar Moghimipour[b,c], Mohsen Rezaei[d], Zahra Ramezani[b] and Farid Abedin Dorkoosh[a,e]

[a]Medical Biomaterial Research Centre (MBRC), Tehran University of Medical Sciences, Tehran, Iran; [b]Nanotechnology Research Center, Ahvaz Jundishapur University of Medical Sciences, Ahvaz, Iran; [c]Cellular and Molecular Research Center, Ahvaz Jundishapur University of Medical Sciences, Ahvaz, Iran; [d]Department of Toxicology, Faculty of Medical Sciences, Tarbiat Modares University, Tehran, Iran; [e]Department of Pharmaceutics, Faculty of Pharmacy, Tehran University of Medical Sciences, Tehran, Iran

ABSTRACT

5-Fluorouracil (5-FU) is one of the most widely used agents in the first-line chemotherapy for colon cancer. However, clinical use of 5-FU is limited because of the low efficacy of drug uptake and systemic toxic effects. Therefore, there is a critical need to find better drug delivery systems in order to improve the efficacy of the drug. In the present study, we have developed a novel combination drug delivery system based on PHBV/PLGA NPs for delivery of 5-FU to cancer cells. NPs were prepared by the double emulsion method and their optimization of preparation was evaluated using Box–Behnken design (BBD) of response surface methodology (RSM). 5-FU loaded NPs were characterized by scanning electron microscope (SEM), differential scanning calorimetry (DSC), thermogravimetry analysis (TGA), and Fourier transformed infra-red spectroscopy (FT-IR). SEM image implied that NPs were spherical in shape and the results of DSC, TGA, and FT-IR suggest that 5-FU was encapsulated into NPs. The obtained results revealed that 5-FU loaded PHBV/PLGA NPs induced significant higher cell death at concentration much lower than free 5-FU. Results of hemolysis assay indicated that the NPs were hemo-compatible. *In vivo* anti-tumor studies showed that 5-FU loaded NPs reduced tumor volume significantly in comparison with free 5-FU. As the first example of using PHBV/PLGA as nano-drug delivery system with enhanced anti-tumor activities, this study establishes PHBV/PLGA as a novel promising drug delivery platform for treatment of colon cancer.

ARTICLE HISTORY
Received 20 June 2019
Revised 21 October 2019
Accepted 22 October 2019

KEYWORDS
5-Fluorouracil; poly (3-hydroxybutyrate-*co*-3-hydroxyvalerate acid); poly (lactic-*co*-glycolic acid); nanoparticles; cancer

1. Introduction

Colon cancer is a major cause of morbidity and mortality all around the world (Xiao et al. 2015). It is the third most common cancer and the fourth most common cause of death (Haggar and Boushey 2009). 5-Fluorouracil (5-FU), an analogue of uracil, is one of the most popular anticancer drugs which is used in the treatment of colon cancer. The drug interferes with DNA synthesis by blocking the thymidylate synthetase (Nair et al. 2011). However, its medical application is limited by short half-life of 10–20 min as well as toxic side effects on the gastrointestinal tract and bone marrow (Chaturvedi et al. 2011; Nair et al. 2011). Various novel drug delivery systems such as liposomes, dendrimers, polymeric nanoparticles (NPs), carbon nanotubes, and nano-emulsions have been reported to overcome the limitations (Yadav et al. 2010; Acharya and Sahoo 2011). Encapsulation of 5-FU in NPs would not only effectively decrease the side effects, but also provide an efficient therapy for colon cancer with reducing dose. NPs are extensively considered as drug delivery system for the diagnosis and treatment of disease (Gao et al. 2013). Among the nanocarriers, polymeric NPs offer exceptional advantages over the other carrier systems due to higher stability in biological fluids, more chemical and physical stability, protection of encapsulated drugs from enzymatic degradation, ability to be freeze-dried for long-term storage, sustained release, ease of modifying properties and capability to entrap small and macromolecules (Yadav et al. 2010; Patel et al. 2014, 2016). Moreover, due to leaky tumor blood vessel around the tumor, NPs can easily penetrate through the vasculature and accumulate in the solid tumors (Matsumura and Maeda 1986; Nair et al. 2011).

Poly (3-hydroxybutyrate-co-3-hydroxyvalerate) (PHBV) is a natural biodegradable polymer, non-toxic and biocompatible with a low production cost that obtained from large-scale bacterial or eukaryotic cells. PHBV has been intensively investigated as a biomaterial for tissue engineering and for drug delivery system (Zhu et al. 2009; Vilos et al. 2013; Penaloza et al. 2017). R-3-hydroxybutyric acid is the main degraded product of PHBV which is a normal ingredient of the blood. Besides, the compound is found in the eukaryotes; therefore, it was supposed that PHBV can be well tolerated *in vivo* (Simion et al. 2013). Unlike poly (lactic-co-glycolic acid) (PLGA), PHBV does not produce acidic degradation products which may be damaging for human tissues (Li et al. 2016). However, it has been reported that entrapment of hydrophilic molecules in PHBV NPs is low (Zhu et al. 2009). On the other hand, it has been demonstrated that PLGA NPs have ability to encapsulate drugs with higher encapsulation efficiency (Zhu et al. 2009). PLGA is extensively used as drug delivery system for a wide range of drugs, including 5-FU due to biocompatibility, biodegradability and possess low toxicity (Coimbra et al. 2008; Gunday Tureli et al. 2016). Some studies have reported that the use of PLGA NPs lead to improving anti-tumor activity of 5-FU

CONTACT Farid Abedin Dorkoosh dorkoosh@tums.ac.ir Department of Pharmaceutics, Faculty of Pharmacy, Tehran University of Medical Sciences, Tehran, Iran

against cancer cells. It was observed that 5-FU loaded PLGA NPs can keep releasing slowly for about 5 days. Cytotoxic studies also confirmed that inhibition effects of 5-FU NPs were more effective than 5-FU solution on cancer cells (Tang et al. 2014). Other researchers have developed 5-FU loaded PLGA NPs in order to overcome the side effects associated with overdosing. Their results showed that 5-FU loaded PLGA NPs had more anti-tumor efficacy with lower dose than free drug (Nair et al. 2011). In another investigation, it was found that 5-FU loaded PLGA exhibited sustained-release *in vitro* and *in vivo*. In addition, 5-FU microsphere could inhibit tumor growth in rabbits more than rabbits which received 5-FU solution. These researches indicated that the PLGA microsphere enhanced the drug concentration in the cancer tissues and also reduced the 5-FU toxicity in normal tissues (Lin et al. 2014).

The aim of this study is to establish a novel promising drug delivery platform based on PHBV/PLGA for treatment of colon cancer. In order to preserve the good biocompatibility of PHBV and to improve the encapsulation efficiency, in the investigation, PHBV/PLGA NPs were selected as drug delivery system for 5-FU. NPs were optimized using design of experiments by employing response surface methodology (RSM). RSM is a collection of mathematical and statistical methods which determine modeling and analysis interactions between the response and the independent variables. This is extensively used in the pharmaceutics including the preparation of NPs carriers (Yu et al. 2014). The Box Behnken experimental design (BBD) of RSM was employed in order to optimize 5-FU loaded NPs. Furthermore, the efficacy and cytotoxicity of drug-loaded NPs were evaluated *in vitro* and *in vivo*.

2. Material and methods

5-Fluorouracil (5-FU) was purchased from Acros, USA. Poly (3-hydroxybutyrate-co-3-hydroxyvalerate acid) (PHBV) containing 2-3% polyhydroxyvalerate (PHV) by weight was obtained from Tianan Biologic Materials Ltd., Hangzhou, China. Poly (lactic-co-glycolic acid) (PLGA, 50:50), polyvinyl alcohol (PVA), 4, 6-diamidino-2-phenylindole (DAPI), paraformaldehyde and 5 (6)-carboxyfluorescein (CF) were acquired from Sigma-Aldrich, Germany.

HT-29 (human colorectal adenocarcinoma) was purchased from Iranian Biological Resource Center (IBRC). CT26 (murine colon carcinoma) was obtained from National Cell Bank of Iran (NCBI), Pasteur Institute of Iran. Dulbecco's modified eagle's medium (DMEM) and fetal bovine serum (FBS) were purchased from Gibco, USA. Penicillin–streptomycin was provided from Sigma-Aldrich, Germany. Male BALB/c mice and male Wistar rats were obtained from the Pasteur Institute of Iran. Other chemicals and solvents were of analytical grade and purchased from Merck, Germany.

2.1. Experimental design

In the present study, Box–Behnken design (BBD) of RSM was used to evaluate the effect of independent variables including PHBV/PLGA ratio (X_1), polymers concentration (X_2) and PVA concentration (X_3) on the encapsulation efficiency (EE%) of 5-FU (Y_1) and particle size (PZ) (Y_2) of NPs (Kudarha et al. 2015). The variables and their levels are presented in Table 1. Experimental factors and their levels were determined according to the preliminary studies. The data of the experiment were assayed by the Design-Expert® software (version 7.0.0, stat-Ease, Inc., Minneapolis, MN) and the 3D response surfaces were also generated in order to demonstrate the relationship and interaction between the variables and responses. According to the BBD, 17 runs were required to reach optimize conditions for the preparation of NPs. Significance of the variables on the responses and the model was found by ANOVA test (p value < 0.05). The adequacy of the model was evaluated by the correlation coefficients (R^2) and adjusted R^2. The optimized predicted formulation was prepared and the actual results were compared with the predicted values.

Table 1. Variables and their levels in BBD.

			Levels	
Independent variables	Factors	Units	Low	High
X_1	PHBV/PLGA ratio		1	3
X_2	Polymer concentration	%	0.5	2.5
X_3	PVA	%	0.25	2
Dependent variables	Units	Constrains		
Y_1	%	Maximum		
Y_2	nm	Minimum		

2.2. Preparation of 5-FU loaded PHBV/PLGA NPs

5-FU loaded PHBV/PLGA NPs were prepared by the double emulsion ($W_1/O/W_2$) method. Briefly, 5-FU (3 mg/mL) was added drop wise into PHBV/PLGA dissolved in chloroform using homogenizer with 20 000 rpm (SilentCrusher M, Heidolph, Germany) to form the primary emulsion (W_1/O). This primary emulsion was then added to an aqueous phase (W_2) containing PVA as emulsifier, which was homogenized again. This emulsion was stirred to completely evaporate the solvent and resulting suspension was centrifuged at 15 000 rpm for 30 min (MPW-350R, Poland). Then NPs were washed three times with distilled water and subsequently freeze-dried at −50 °C for 24 h (Operon, Korea) for further experiments. The schematics preparation of NPs is shown in Figure 1.

2.3. Determination of encapsulation efficiency

The suspension obtained after solvent evaporation was centrifuged and the amount of free 5-FU in the supernatant was determined using high-performance liquid chromatography (HPLC, Waters, USA) at a detection wavelength of 260 nm. C_{18} column (250 × 4mm i.d., 5 μm) was employed for the measurements. The mobile phase was composed of 0.02 M phosphate buffer (pH 4) and methanol (70:30, V/V) at a flow rate of 0.8 ml/min. Analysis temperature was set as 30 °C and the sample injection volume was 50 μL. Encapsulation efficiency (EE%) was calculated using the Equation (1):

$$EE\% = (D_t - D_f/D_t) \times 100 \quad (1)$$

where D_f is the amount of remained free 5-FU in supernatant and D_t is the initial added amount of the drug. Drug loading (DL%) was also determined according to the following Equation (2):

$$DL\% = (D_t - D_f/W) \times 100 \quad (2)$$

where D_f is the amount of remained free 5-FU in supernatant, D_t is the initial added amount of the drug, and W is the Weight of NPs.

2.4. Particle size determination and morphological studies

The particle size of 5-FU loaded PHBV/PLGA NPs was determined by particle sizer (Qudix, ScatterOScope I, Korea) system at 25 °C. The obtained NPs were diluted in deionised water and sonicated in ultrasonic bath (Elma, Germany) before the measurement for

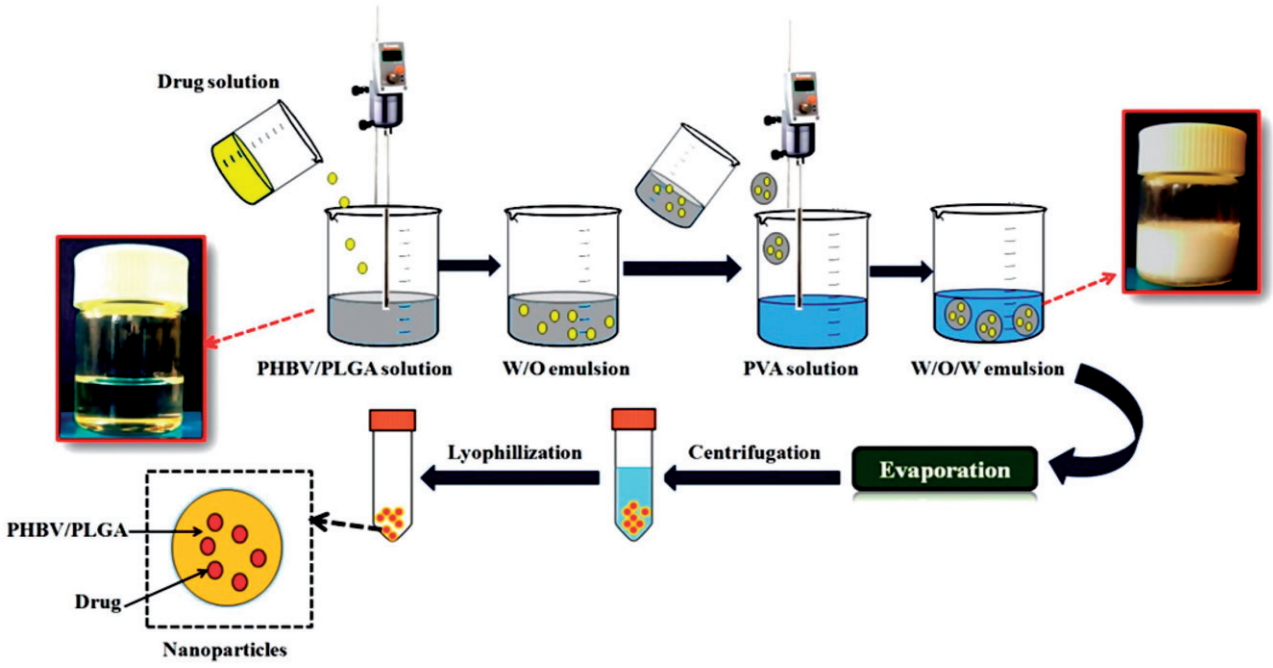

Figure 1. Schematic representation of 5-FU loaded PHBV/PLGA NPs.

preventing particles agglomeration. The morphology of 5-FU loaded PHBV/PLGA NPs was also examined by field emission scanning electron microscopy (FESEM, S4160, and Hitachi, Japan).

2.5. Differential scanning calorimetry

Thermal behavior of PHBV, PLGA, 5-FU, and 5-FU loaded PHBV/PLGA NPs was performed using a differential scanning calorimeter (DSC-1 Mettler Toledo, Switzerland). 5 mg of each sample were sealed in aluminum pans and heated from 0 to 300 °C for 30 min at a rate of 10 °C/min.

2.6. Thermogravimetry analysis

Thermogravimetry analysis (TGA) was carried out with simultaneous thermal analyzer STA503 (BÄHR-Thermoanalyse GmbH, Germany). The lyophilized PHBV/PLGA NPs and 5-FU loaded PHBV/PLGA NPs were weighted and heated from 0 to 600 °C under nitrogen pressure.

2.7. Fourier transformed infra-red spectroscopy

Fourier transformed infra-red spectroscopy (FT-IR) spectra of PHBV, PLGA, 5-FU, and 5-FU loaded PHBV/PLGA NPs were recorded on a FT-IR spectrometer (Vertey 70, Bruker, Germany). The lyophilized samples were mixed with KBr and prepared as pellets. The spectra were obtained from samples in the range of 400–4000 cm^{-1} at room temperature.

2.8. In vitro *release study*

The *in vitro* release of 5-FU from NPs was carried out using dialysis bags. 1 ml of the NPs formulation and free drug were placed in the dialysis bag (MWCO 12 kDa) and immersed in 10 ml release medium at 37 °C with stirring at 100 rpm. At specified time points, 500 μL of release medium was withdrawn and replaced with fresh medium. The released amount of 5-FU was determined using HPLC as described above.

2.9. In vitro *cellular uptake of NPs*

As 5-FU is a non-fluorescent drug, CF loaded PHBV/PLGA NPs were prepared in order to study the cellular uptake of NPs. HT-29 cells were grown at a density of 1×10^5 cells in 6-well plates and incubated overnight. The culture medium was replaced with growth medium containing free CF and CF loaded PHBV/PLGA NPs and incubated for 4 h at 37 °C. After 4 h, the cells were washed with PBS for three times to eliminate excess of NPs. Then cells were fixed in 4% paraformaldehyde for 15 min and further stained with 4, 6-diamidino-2-phenylindole (DAPI) for 10 min. The intracellular uptake of CF in the cells was observed using fluorescent microscope (Olympus IX71, Japan).

2.10. Cytotoxicity assay

The MTT method was used for the assessment of cytotoxic effects. MTT is a yellow compound that cleavages by mitochondrial enzymes and produces purple formazan crystals. HT-29 cells were grown in DMEM supplemented with 10% FBS and 1% penicillin–streptomycin. The cultures were kept in a humidified incubator with 5% CO_2 at 37 °C for 24 h. HT-29 cells were then seeded at a density of 1×10^4 cells/well in a 96-well culture plate and allowed to attach and grow for 24 h. After overnight incubation, cells were treated with different concentrations of 5-FU and 5-FU loaded PHBV/PLGA NPs (25, 35, 50, 75 and 100 μM) for 48 h. After 48 h, 20 μL of MTT solution (5 mg/mL) was added to each well and incubated for 4 h at 37 °C. Then 100 μL of DMSO was added per well to solubilize the formazan crystals. The optical density of each well was analyzed by ELISA reader at 570 nm (BioRad, USA) and the survival rates were calculated by the following Equation (3):

$$\text{Cell viability } \% = (\text{Abs}_{\text{sample}}/\text{Abs}_{\text{control}}) \times 100 \quad (3)$$

According to the cell viability values, concentration inhibiting half of the cells (IC_{50}) was also calculated.

2.11. Hemolysis assay

Hemolytic test was employed to evaluate the compatibility of NPs with the red blood cells (RBC). RBCs of male Wistar rats were collected by centrifugation at 1500 rpm/min for 10 min and then washed three times using PBS. The empty PHBV/PLGA NPs and 5-FU loaded PHBV/PLGA NPs (1 mg/mL) were added in RBC suspension and incubated for 3 h at 37 °C. Then, the mixtures were centrifuged at 1500 rpm for 10 min, the supernatant was collected and the absorbance was read in a spectrophotometer (Biochrom WPA biowave II, England) at 540 nm. H_2O and PBS were used as positive and negative controls, respectively. The percentage of hemolysis was calculated by the following formula (4):

$$\text{Hemolysis (\%)}: \quad (A_s - A_{nc}/A_{pc} - A_{nc}) \times 100 \tag{4}$$

where A_s is the absorbance of sample, A_{nc} is the absorbance of negative control, and A_{pc} is the absorbance of positive control.

2.12. In vivo *anti-tumor activity*

BALB/c mice were employed in the experiments and all animal procedures were performed according to the Animal Ethics Committee Jundishapur University of Medical Sciences, Ahvaz, Iran (ref no. IR.AJUMS.REC.1395.643). The mice were subcutaneously injected at the right axillary space with 0.1 ml of cell suspension containing 1×10^6 CT26 cells. When the tumor volume reached to 100 mm^3, the mice were randomly divided into three groups ($n = 5$): control, 5-FU, and 5-FU loaded PHBV/PLGA NPs. Mice received 6 injections every other day *via* intraperitoneally at a 5-FU dose of 20 mg/kg for a treatment period of 12 days. The dosage of drug administered was accorded to the literature (Le et al. 2015). The tumor volume and body weight were measured simultaneously. Tumor size was measured by caliper and the volume of tumors was calculated using the following formula (5):

$$V = (W^2 \times L)/2 \tag{5}$$

where L is the longest diameter and W is the shortest diameter. On day 21 after tumor inoculation, the mice were sacrificed and the tumors were excised and photographed.

2.13. Statistical analysis

The results were presented as mean ± SD. The statistical differences were performed using one-way analysis of variance (ANOVA). A p value less than 0.05 was considered as statistically significant.

3. Results and discussion

3.1. Design experimental

One of the important advantages of applying RSM is a considerable reduction of the number of experimental runs (Feczkó et al. 2011). In the study, BBD which is one of the common experimental design method used in RSM was employed to achieve the exact relationship between variables for finding the optimal response (Huang et al. 2014). 17 experiments were conducted by BBD and the values of independent variables and responses are shown in Table 2.

Table 2. BBD experimental runs and acquired responses.

Run	PHBV/PLGA ratio	Con.polymer (%)	PVA (%)	EE (%)	PZ (nm)
1	1.00	0.50	1.13	21.3166 ± 0.01	169 ± 2.98
2	1.00	2.50	1.13	39.7612 ± 0.12	673 ± 1.54
3	2.00	2.50	0.25	28.1774 ± 0.24	318 ± 1.08
4	3.00	1.50	2.00	53.8616 ± 0.04	78 ± 2.07
5	2.00	1.50	1.13	33.6139 ± 1.23	335 ± 2.65
6	3.00	1.50	0.25	27.3921 ± 0.52	294 ± 1.04
7	2.00	0.50	0.25	9.50734 ± 0.06	181 ± 1.85
8	3.00	0.50	1.13	14.0105 ± 0.37	168 ± 2.23
9	2.00	1.50	1.13	28.8865 ± 0.61	435 ± 2.95
10	3.00	2.50	1.13	39.484 ± 0.76	98.9 ± 1.62
11	2.00	0.50	2.00	32.1505 ± 1.01	66.7 ± 1.93
12	1.00	1.50	0.25	24.6593 ± 1.21	216 ± 2.01
13	2.00	2.50	2.00	47.925 ± 0.07	684 ± 2.61
14	1.00	1.50	2.00	39.8405 ± 0.91	668 ± 1.72
15	2.00	1.50	1.13	30 ± 0.65	500 ± 1.47
16	2.00	1.50	1.13	22.2169 ± 0.84	430 ± 1.12
17	2.00	1.50	1.13	28.7 ± 1.67	437 ± 1.93

Table 3. The analysis of variances for EE% as the response (Y_1) ($n = 3$).

Source	Sum of squares	df	Mean squares	F-value	p-value*
Model	1882.59	9	209.18	9.56	0.0035
X_1	10.51	1	10.51	0.48	0.5106
X_2	767.59	1	767.59	35.07	0.0006
X_3	882.87	1	882.87	40.33	0.0004
X_1X_2	12.35	1	12.35	0.56	0.4770
X_1X_3	31.86	1	31.86	1.46	0.2669
X_2X_3	2.10	1	2.10	0.096	0.7660
X_1^2	50.96	1	50.96	2.33	0.1709
X_2^2	52.15	1	52.15	2.38	0.1666
X_3^2	76.98	1	76.98	3.52	0.1029
Residual	153.23	7	21.89		
Lack of fit	85.33	3	28.44	1.68	0.3082
Pure error	67.90	4	16.98		
Cor. total	2035.82	16			
R^2	0.9247				
Adjusted R^2	0.8280				

*Confidence level at $p = 0.05$.

According to the results analysis of variance for EE% as a response (Table 3), a quadratic second-order polynomial Equation (6) was fitted as below:

$$\begin{aligned} Y_1 = {} & +22.38922 - 19.03379(X_1) + 17.76962(X_2) \\ & -5.76958(X_3) + 1.75723(X_1X_2) + 3.22522(X_1X_3) \\ & -0.82731(X_2X_3) + 3.47896(X_1)^2 - 3.51934(X_2)^2 + 5.58490(X_3)^2 \end{aligned} \tag{6}$$

where Y_1 is the predicted EE% and X_1, X_2, and X_3 are PHBV/PLGA ratio, polymers concentration, and PVA concentration, respectively. As shown in Table 3, the lack of fit of the obtained equation is not significant (F-value = 1.68; p value = 0.3082). The 'lack of fit F-value' of 1.68 implies the lack of fit is not significant relative to the pure error. There is a 30.82% chance that a 'lack of fit F-value' this large could occur due to noise. Lack of fit should be non-significant for the model to fit (Zeng et al. 2016). Low p-value of the model ($p < 0.05$) also confirmed that the model can significantly represent the actual relationship between factors and response. Furthermore, for the good fit of a model, coefficient of determination (R^2) should be 0.80 or higher which indicates the adequacy of the applied model (Zeng et al. 2016). The value of R^2 and adjusted R^2 of this equation were 0.92 and 0.82, respectively. The proximity between R^2 and adjusted R^2 indicated the good correlation between the response and the selected variables.

Table 4. The analysis of variances for NPs size as the response (Y_2) ($n = 3$).

Source	Sum of squares	df	Mean squares	*F*-value	*p* value*
Model	6.652E + 005	9	73913.66	18.99	0.0004
X_1	1.477E + 005	1	1.477E + 005	37.95	0.0005
X_2	1.768E + 005	1	1.768E + 005	45.42	0.0003
X_3	29731.41	1	29731.41	7.64	0.0279
X_1X_2	82110.90	1	82110.90	21.10	0.0025
X_1X_3	1.116E + 005	1	1.116E + 005	28.66	0.0011
X_2X_3	57672.02	1	57672.02	14.82	0.0063
X_1^2	23244.17	1	23244.17	5.97	0.0445
X_2^2	24240.07	1	24240.07	6.23	0.0413
X_3^2	6437.09	1	6437.09	1.65	0.2393
Residual	27245.76	7	3892.25		
Lack of fit	13280.56	3	4426.85	1.27	0.3980
Pure error	13965.20	4	3491.30		
Cor. total	6.925E + 005	16			
R^2	0.9607				
Adjusted R^2	0.9101				

*Confidence level at $p = 0.05$.

The results obtained from the analysis of variance for particle size as the response are shown in Table 4. A quadratic second-order polynomial model is the best fitted model for particle size with the following Equation (7):

$$Y_2 = -762.41416 + 590.93929(X_1) + 508.44286(X_2) + 360.44898(X_3) - 143.27500(X_1X_2) - 190.85714(X_1X_3) + 137.22857(X_2X_3) - 74.30000(X_1)^2 - 75.87500(X_2)^2 - 51.06939(X_3)^2 \quad (7)$$

where Y_2 is the particle size and X_1, X_2, and X_3 are PHBV/PLGA ratio, polymers concentration, and PVA concentration, respectively. The lack of fit of the model was not significant (*F*-value = 1.27; *p* value =0.3980). The R^2 and adjusted R^2 of this model were predicted to be 0.96 and 0.91, respectively. This R^2 illustrates that 96% of variability in the response could be explained by the model. On the other hand, the similarity between R^2 and adjusted R^2 confirmed the efficiency of the model to predict particle size by the optimized method.

The 3D response surface plot of EE% and particle size is shown in Figure 2(A–F). As shown in Figure 2(A,B), EE% and particle size increased by enhancement the polymers concentration and PHBV/PLGA ratio. This effect can be explained by the fact that increasing the total concentration of the polymers leads to an increase in the viscosity of organic phase, which in turn, prevents drug diffusion from the organic to the inner aqueous phase. Higher polymers concentration also increase polymer–polymer interactions, as a result more polymer chains remain associated during the solvent's diffusion into the aqueous medium (Halayqa and Domańska 2014; Tefas et al. 2015). On the other hand, increasing the viscosity of organic phase reduces the dispersion of organic phase into the aqueous phase, which increases the NPs size (Halayqa and Domańska 2014). Increasing EE% and particle size by increasing polymers ratio can be related to the higher molecular weight of PHBV in comparison to PLGA. The longer carbon chain of PHBV can fabricate larger NPs due to polymer chain entanglement during emulsification which results increasing the EE% and particle size of NPs (Zhu et al. 2009). As illustrated in the Figure 2(C,D), increasing the concentrations of PVA and PHBV/PLGA ratio led to enhance EE% and size of NPs. Moreover, as can be seen from Figure 2(E,F), EE% increased by enhancement the polymers concentration; however, by increasing PVA concentration, EE% and particle size were increased and reduced, respectively. According to the previous reports, PVA at higher concentrations leads to increase density of the aqueous phase and decreases the net shear stress in the emulsification process, which results increasing the NPs size (Halayqa and Domańska 2014). On the other hand, some studies implied that PVA as an emulsifier reduces the superficial tension between organic phase drops and the aqueous phase (Duran et al. 2008), which results in an increasing of the net shear stress and formation of small size NPs during the emulsification process (Galindo-Rodriguez et al. 2004). In the current study, with regarded to the result of optimum formulation (below section), it seems that increasing PVA concentration causes a decrease in size of NPs.

3.2. Optimization and validation of model

The optimized formulation was chosen based on the criteria of achieving maximum EE% and the smallest particle size. The observed responses followed by predicated error values were indicated in Table 5. Regarding the results, the observed amounts were close to the predicted value which confirmed significance and predictability of models. DL% of the optimum formulation was also 2.4%.

3.3. Morphological studies

SEM was carried out in order to achieve information about morphology, aggregation, and size of NPs. As can be seen from Figure 3, NPs were spherical in shape with no particle aggregation. In addition, NPs exhibited a size distribution approximately from 100 to 200 nm which was in close agreement with the value determined by particle analyzer.

3.4. DSC analysis

DSC is a useful method to evaluate the interaction between the drug and NPs and the state of the drug after encapsulation process (Yadav et al. 2010). Thermogram of 5-FU, PHBV, PLGA, and 5-FU loaded NPs are shown in Figure 4(A). The DSC curve of 5-FU displayed an endothermic peak at temperature of 282 °C, corresponding to its melting point and giving the verification for crystal structures of the drug (Figure 4(Aa)). The PHBV and PLGA exhibited endothermic peaks at 177 °C and 48 °C, respectively which were in agreement with the reported data in the literatures (Amjadi et al. 2013; Manoochehri et al. 2013; Kouhi et al. 2015). According to Figure 4(Ab), endothermic peak corresponding to 5-FU was not observed, which suggest that drug may be encapsulated into NPs.

3.5. Thermogravimetry analysis

The presence of 5-FU in NPs was further confirmed by TGA analysis. As shown in Figure 4, three significant events of weight loss were occurred with increasing temperature. While in the 5-FU loaded NPs, the thermogram pattern was not changed significantly but a shift in the temperature (283, 364.4, and 487 °C to 294, 358, and 413 °C, respectively) was observed. Weight loss is also changed from 37.9, 68.2, and 93.1% to 59.3, 79.1, and 83.8%, respectively. This temperature shift may be due to the interaction between drug and polymeric NPs. The increase in weight loss of drug contaning NPs is attributed to the presence of 5-FU in the NPs. The rate of NPs degradation in the temperature range of 230 °C to 490 °C was slower than drug containing NPs. In other words, the loaded drug in the NPs led to decrease the stability of NPs, which may be due to interaction of drug with NPs. Difference in weight loss at temperatures about 480 to 600 °C (about 1% for NPs and 7% for 5-FU loaded NPs) are another indicators of 5-FU loading. Our findings are in agreement with Khan

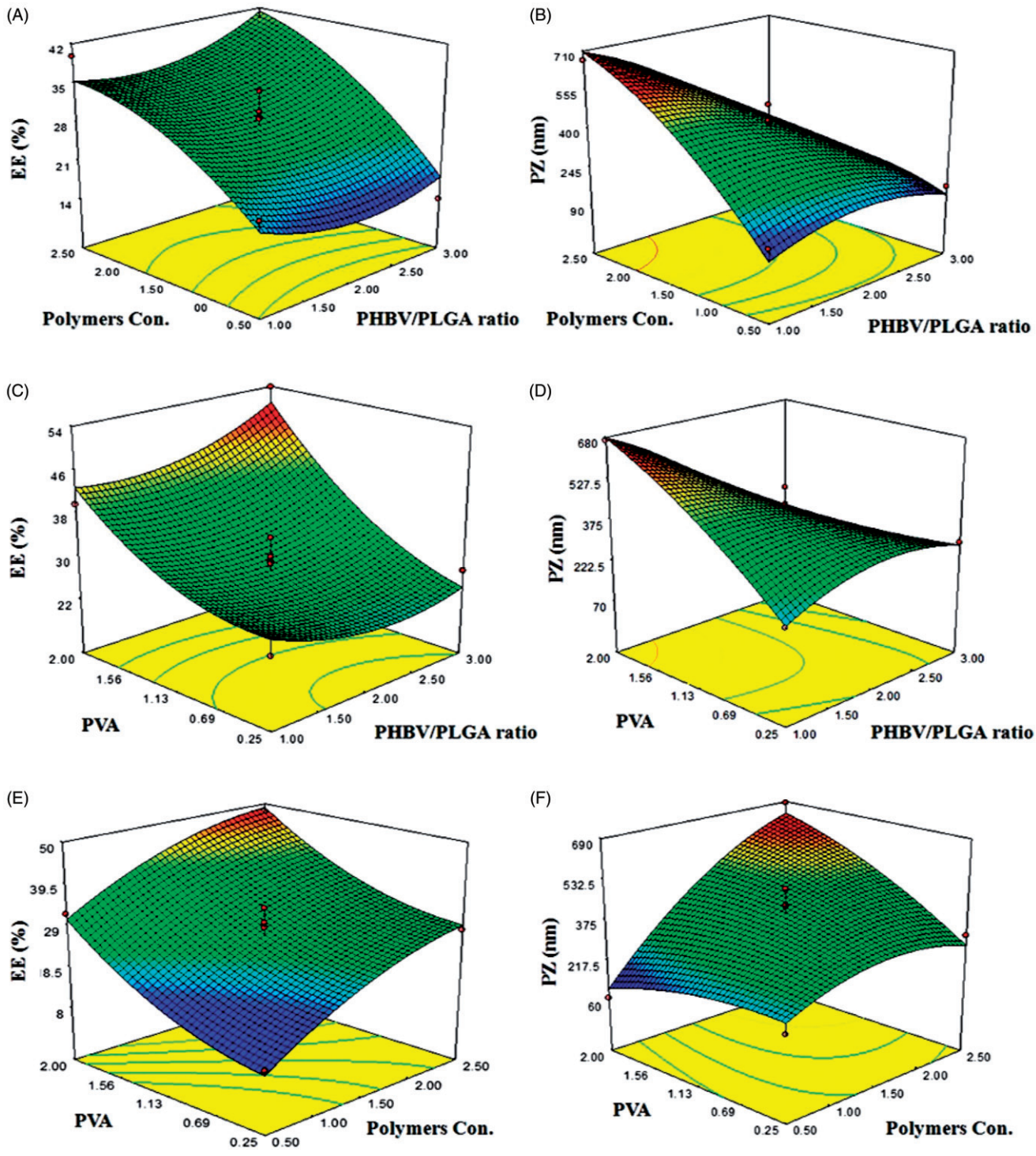

Figure 2. Three-dimensional plots for the effect of polymers concentration and PHBV/PLGA ratio on (A) EE% and (B) PZ; effect of PVA concentration and PHBV/PLGA ratio on (C) EE% and (D) PZ and effect of PVA concentration and polymers concentration on (E) EE% and (F) PZ.

Table 5. Predicted and observed responses obtained at optimum conditions.

Independent variable		Optimized amount	Dependent variable		Predicted amount	Observed amount	Prediction error (%)
X_1	PHBV/PLGA ratio	3	Y_1	EE%	48.72	43.86	−9.98
X_2	Polymer Con.	1.7	Y_2	PZ	144.83	135	−6.77
X_3	PVA	2					

et al. (2015) results. They observed that weight loss of 55% and 80% for PLGA NPs and 74% and 95% for ormeloxifene loaded PLGP NPs. They indicated that greater weight loss was related to the presence of ormeloxifene in the NPs, which confirm the loading of the drug in NPs (Khan et al. 2015). Dubey et al. (2016) also reported that increase in weight loss of PLGA NPs was

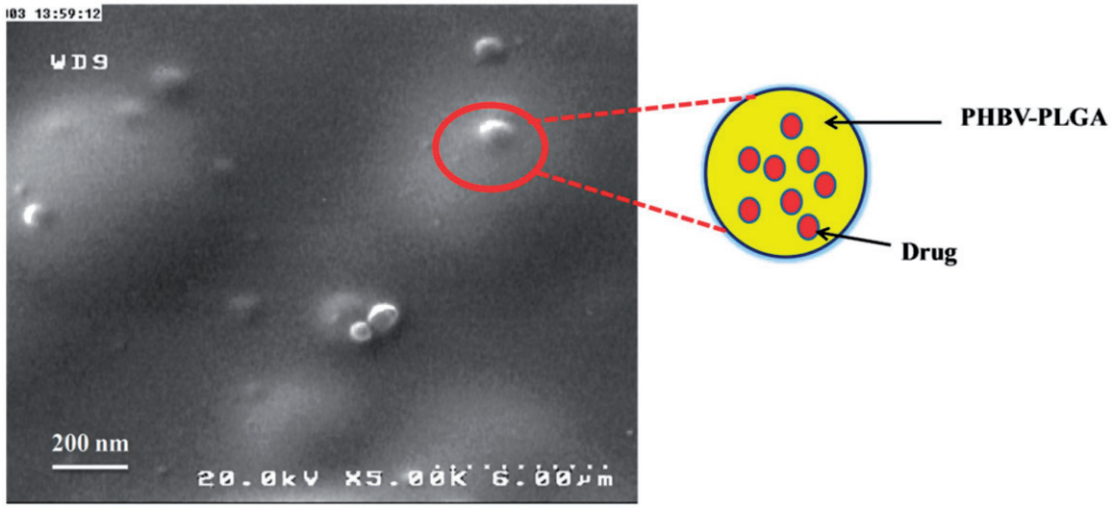

Figure 3. SEM image of 5-FU loaded PHBV/PLGA NPs.

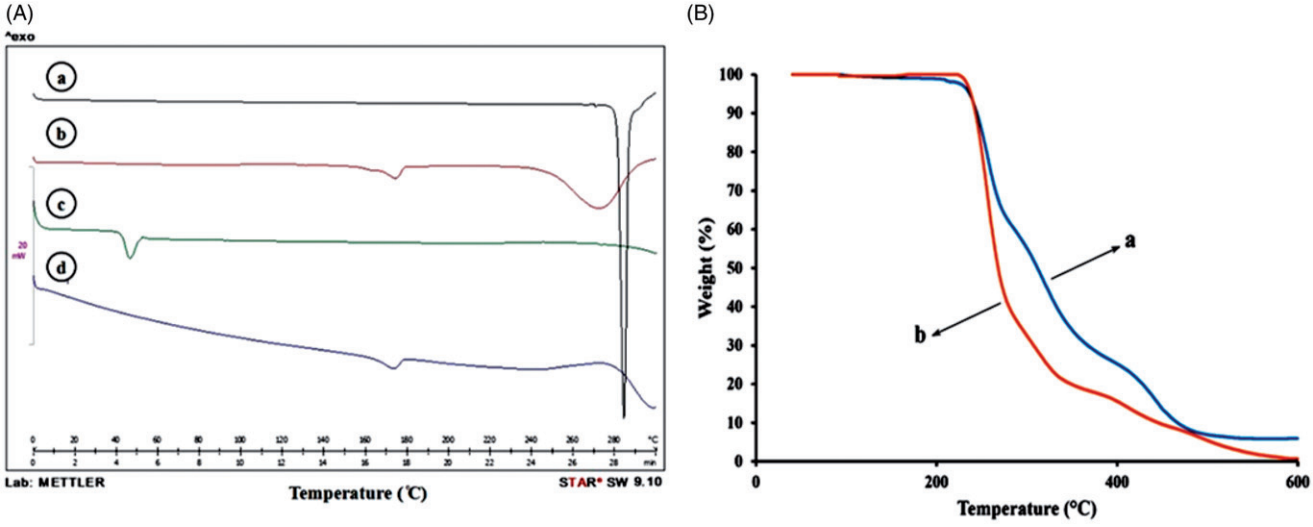

Figure 4. (A) DSC thermograms of (a) 5-FU, (b) 5-FU loaded PHBV/PLGA NPs (c) PLGA and (d) PHBV and (B) TGA curve of (a) blank NPs and (b) 5-FU loaded PHBV/PLGA NPs.

attributed to the presence of pentacyclic triterpenediol in the NPs, confirming the entrapment of the drug in the NPs (Dubey et al. 2016).

3.6. Fourier transformed Infra-Red spectroscopy (FT-IR)

FT-IR spectra of 5-FU, PHBV, PLGA, and 5-FU loaded PHBV/PLGA NPs are shown in Figure 5. As depicted in Figure 5(A), a broad band between the 3000 and 3500 cm^{-1} is attributed to –NH stretching vibrations in the spectrum of 5-FU. The peak at 1662 cm^{-1} is related to the C5 = C6 stretching vibration. A peak at 1242 cm^{-1} is also assigned to C–N stretching. The FT-IR spectrum of PHBV (Figure 5(B)) exhibited a C=O absorption bond of aliphatic ester in 1730 cm^{-1} region with high intensity. The bonds observed in 1380 and 1453 cm^{-1} correspond to the CH_2 group adjacent to the carbonyl group of ester in structure of PHBV. Characteristic bands from 829 to 977 cm^{-1} are corresponded to symmetric –C–O–C– stretching vibration. Similar results were observed by Oner et al. (2016). They expressed that PHBV displayed the band responsible for C=O stretching at 1720 cm^{-1} and various aliphatic C–H vibration bands in the regions 1227–1478 cm^{-1} (Oner et al. 2016). Vilos et al. (2013) also reported that PHBV showed bands at 1680–1725 cm^{-1} which were related to carboxyl groups (Vilos et al. 2013). The FT-IR spectrum of PLGA displayed a strong peak at 1766 cm^{-1} (C=O stretching) which indicating the surface carboxylic groups of PLGA. The peaks at 2960 cm^{-1} and 2996 cm^{-1} are attributed to the C–H stretch of CH_2. A broad band at 3510 cm^{-1} is assigned to OH stretching and the peak at 1092 cm^{-1} is related to C–O–C stretching (Figure 5(C)). This finding is in agreement with observation of Patel et al. (2016) which reported that broad bands 3200–3600 cm^{-1} are related to terminal hydroxyl group (Patel et al. 2016). Amin et al. (2016) indicated that a peak at 1757 cm^{-1} is refereed to carbonyl (C=O) stretching of PLGA (Amin et al. 2016). Dubey et al. (2016) also reported that a sharp peak at 1759 cm^{-1} is correlated to C=O stretching (Dubey et al. 2016). The identical drug peaks were observed in the 5-FU loaded PHBV/PLGA NPs while these peaks were not present in the blank PLGA and PHBV (Figure 5(D)). These results confirmed the incorporation of 5-FU in PHBV/PLGA NPs.

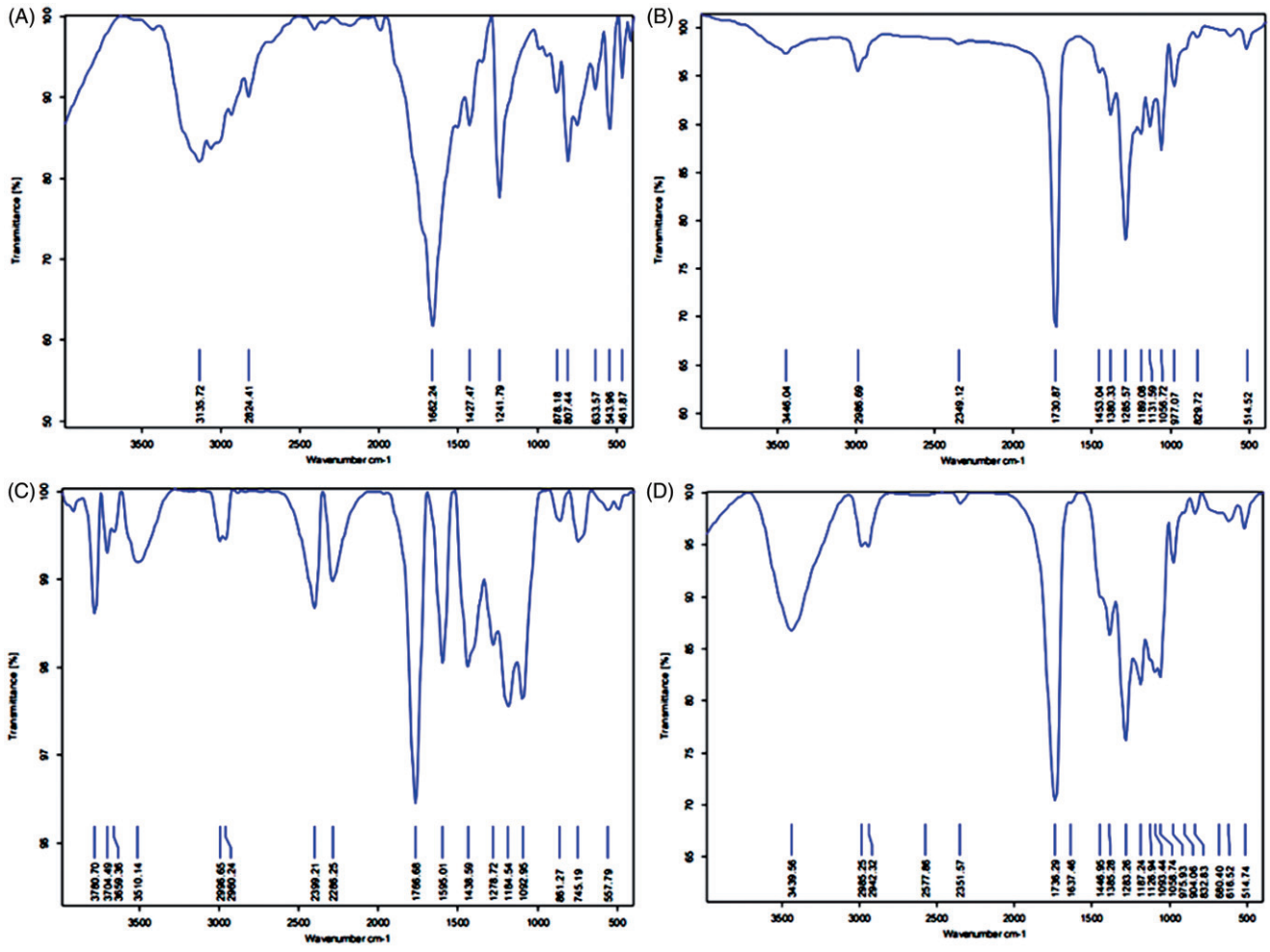

Figure 5. FT-IR spectra of (A) 5-FU, (B) PHBV, (C) PLGA and (D) 5-FU loaded PHBV/PLGA NPs.

3.7. In vitro *release study*

As shown in Figure 6, almost 100% of free 5-FU was released at 4 h; whereas, about 30% of drug leaked from the NPs. On the other word, these results indicated the prolonged and sustained release of 5-FU from NPs. The findings also confirmed that these drug-loaded NPs have potential control effect on the rate of drug release.

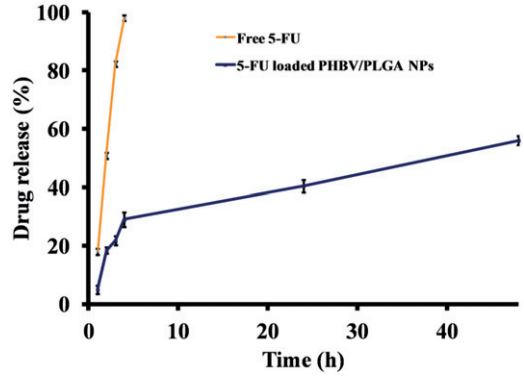

Figure 6. *In vitro* release profile of free 5-FU and 5-FU loaded PHBV/PLGA NPs.

3.8. In vitro *cellular uptake of NPs*

The intracellular uptake of NPs was evaluated by encapsulating CF in PHBV/PLGA NPs. In order to contrast to the green color of CF, nuclei were stained with DAPI which appear in blue. The selection of the fluorescent dye was based on the similarity of the physicochemical properties with drug. According to Figure 7(A,B), CF-loaded NPs were internalized more effectively compared with the free CF. These findings demonstrated that the NPs enhance delivery of drugs into cancer cells. CF is hydrophilic molecule and it is established that hydrophilic molecules have low intracellular absorption (Eloy et al. 2014). NPs can release their cargo directly in the cells and can improve the low cellular uptake of hydrophilic drugs (Sadhukha and Prabha 2014). The present results are in accordance with observation of Sadhukha and Prabha (2014), which showed that carboplatin (a hydrophilic drug) loaded PLGA NPs were taken up by the cells efficiently more than free drug (Sadhukha and Prabha 2014). The enhanced internalization of CF-loaded PHBV/PLGA NPs may confirm the hypothesis that NPs are taken up by endocytosis. It is believed that endocytosis is one of the principal mechanisms for the uptake of NPs (Zeng et al. 2014). Penaloza et al. (2017) indicated that PHBV NPs are taken up by endocytosis pathway in the HeLa cells (Penaloza et al. 2017). It has also been reported that endocytosis is a major pathway in the uptake of PLGA NPs (Acharya and Sahoo 2011). Moreover, our results confirmed the biocompatibility of PHBV/PLGA NPs because efficient cellular uptake was observed. The proposed mechanism of endocytosis uptake of NPs is shown schematically in Figure 7.

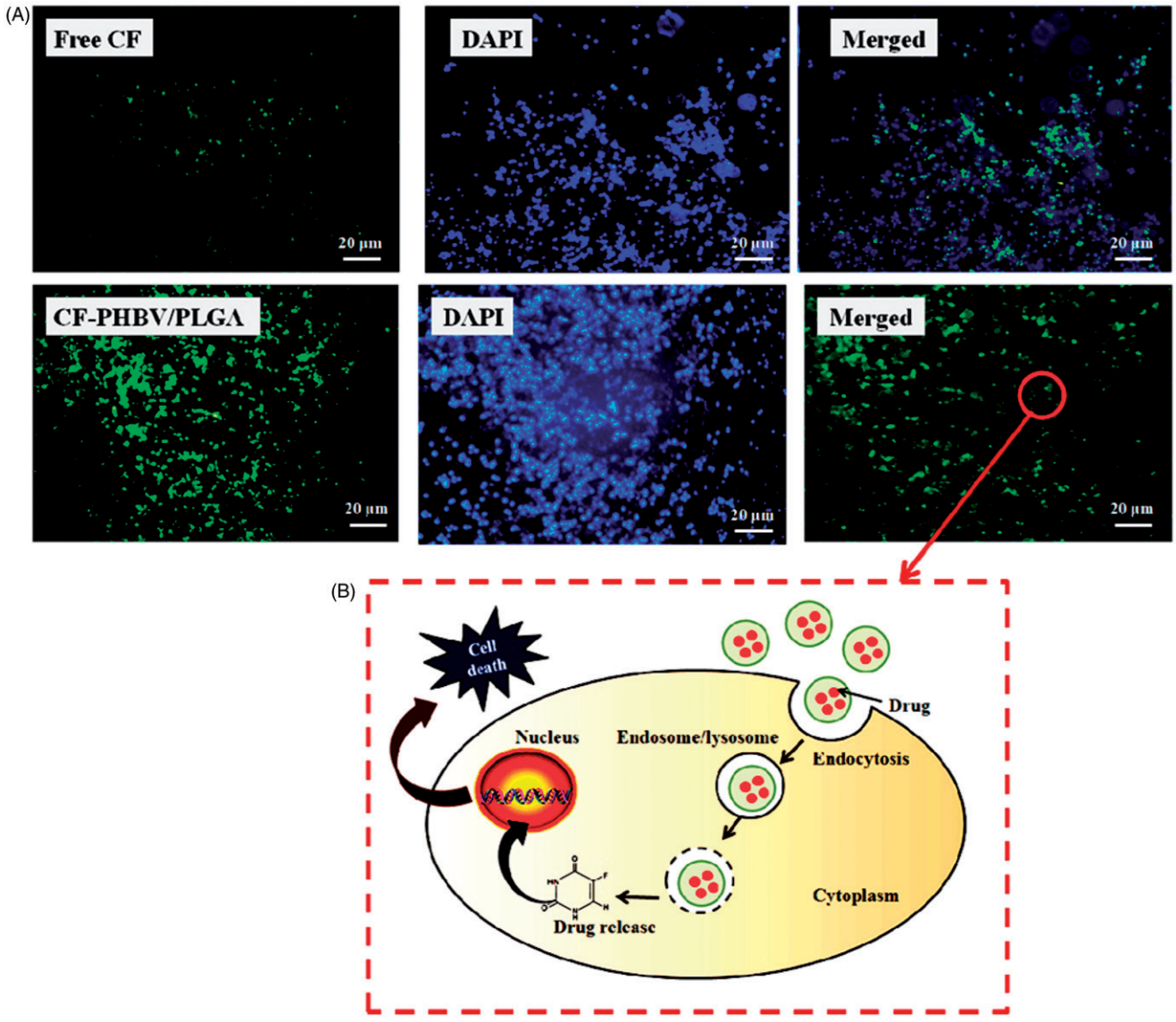

Figure 7. Cellular uptake of (A) free CF and (B) CF loaded PHBV/PLGA NPs (Scale bar = 20 µm).

3.9. Cytotoxicity assay

In vitro cytotoxicity of 5-FU and 5-FU loaded NPs was evaluated by MTT method. As shown in Figure 8, drug-loaded NPs exhibited higher cytotoxicity than free drug ($p < 0.05$). In addition, anticancer activity of free 5-FU and 5-FU loaded NPs were concentration dependent. The IC_{50} values for 5-FU and 5-FU loaded NPs were 107.15 and 46.77 µM, respectively. The higher cytotoxicity of drug loaded NPs may be related to the higher cellular uptake *via* endocytosis, higher intercellular delivery of drug and greater distribution into the cells (Dadashzadeh et al. 2008; Sadhukha and Prabha 2014); while, free 5-FU absorbs poorly and washes out rapidly due to its hydrophilic nature (Mattos et al. 2016). These findings are in agreement with Joshi et al. (2014) results which reported that the gemcitabine HCl loaded PLGA NPs had a significantly higher cytotoxicity than free drug. Moreover, they indicated that higher cytotoxic effect of PLGA NPs is related to higher uptake of NPs through endocytosis and greater internalization in comparison to free drug which is not internalize owing to its hydrophilicity (Joshi et al.

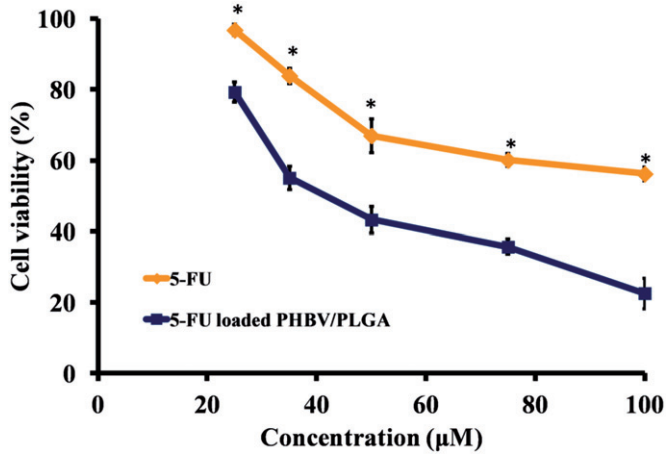

Figure 8. Cytotoxicity effect of free 5-FU and 5-FU loaded PHBV/PLGA NPs on the HT-29 cells (*Significant different with 5-FU loaded PHBV/PLGA). Data were given as mean ± SD ($n = 3$).

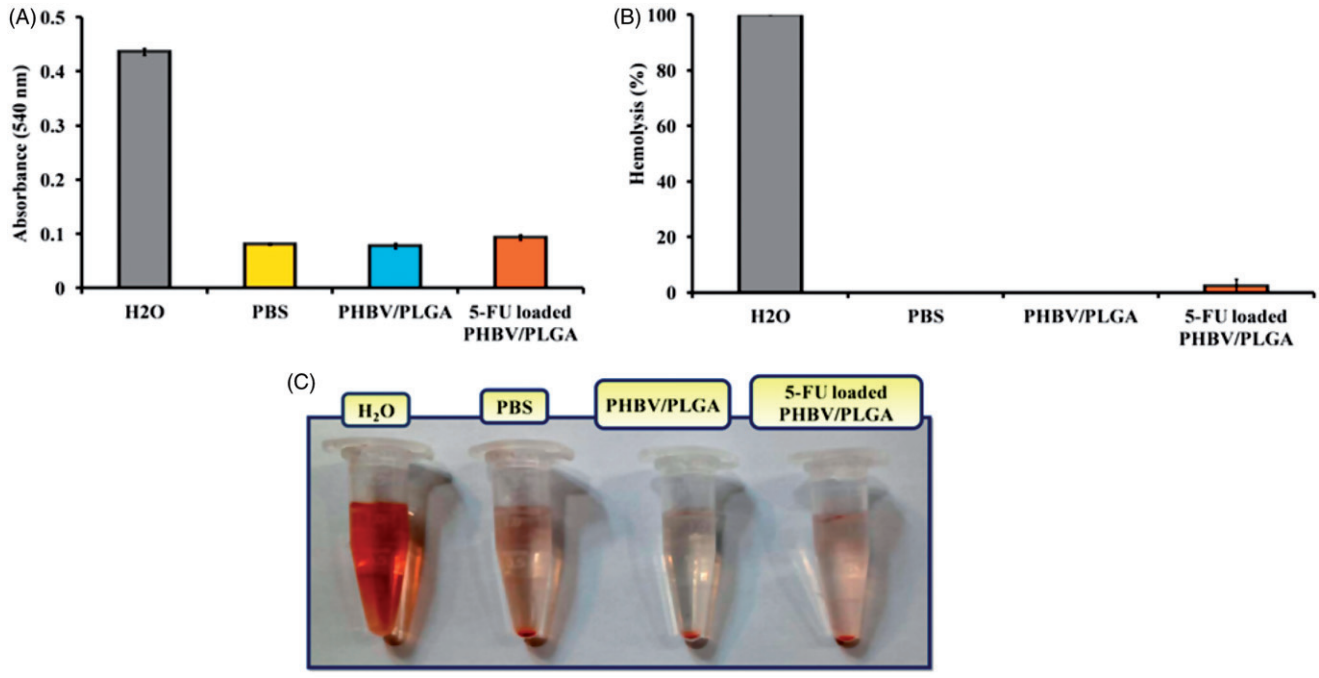

Figure 9. Hemolysis assay: (A) absorbance value, (B) hemolysis (%) and (C) image of RBCs treated with H_2O, PBS, PHBV/PLGA NPs and 5-FU loaded PHBV/PLGA NPs.

2014). expressed that resveratrol containing NPs exhibited better cytotoxicity than the free resveratrol on the human hepatocarcinoma cells (Huang et al. 2017). Similar results were observed in the study of Nair et al. (2011) which reported that 5-FU loaded PLGA NPs showed higher toxicity than free 5-FU against MCF-7 cells (Nair et al. 2011). Jain et al. (2011) implied that the cell viability of breast cancer cells was relatively lower in tamoxifen loaded PLGA NPs treated cells as compared to free tamoxifen treated cells (Jain et al. 2011). Masood et al. (2013) also found that ellipticine loaded PHBV NPs inhibited the growth of cancer cells approximately two fold higher in comparison to free drug. They implied that PHBV NPs have a great potential to increase the cytotoxic effect of anticancer drugs and are a promising strategy for cancer therapy (Masood et al. 2013).

3.10. Hemolysis assay

Detection of NPs hemolytic potential is an important step in evaluation biocompatibility of NPs (Dobrovolskaia and McNeil 2013). Therefore, we performed the hemolysis analysis to investigate the blood compatibility of PHBV/PLGA NPs. The value of absorbance, hemolysis percentage and image of RBCs treated with H_2O (as positive control), PBS (as negative control), PHBV/PLGA NPs, and 5-FU loaded PHBV/PLGA NPs are illustrated in Figure 9(A–C). The results showed that PHBV/PLGA NPs did not induce hemolysis. The hemolysis percentages of 5-FU loaded PHBV/PLGA NPs were lower than 5%. Commonly, hemolysis percentage of $<5\%$ is considered as nontoxic and safe (Yang et al. 2016). As shown in Figure 9(C), PBS and H_2O led to no visible and total hemolysis of RBC, respectively. According to the results, PHBV/PLGA NPs exhibited good hemo-compatibility. Therefore, they can be employed as suitable candidates for drug delivery. Similar observations were reported by Yadav et al. (2010) which found that 5-FU loaded PLGA NPs were hemo-compatible (Yadav et al. 2010). Mendes et al. (2012) also observed that PHBV/PCL microparticles had no cytotoxic effect on RBC which confirms their potential for pharmaceutical applications (Mendes et al. 2012).

3.11. In vivo *anti-tumor activity*

As shown in Figure 10(A), the tumor volumes in mice that received 5-FU loaded PHBV/PLGA NPs was significantly lower than control groups and groups treated with the free drug ($p < 0.05$, except for the first two days of treatment period). Moreover, at first, the free 5-FU had negligible effect on tumor growth; however, at the end of the treatment period, a significant difference was observed between the treatment groups and the control groups. These results indicate that the *in vivo* antitumor activity of 5-FU was remarkably enhanced after encapsulation in the polymeric NPs. No significant change in the body weight was observed between the treated groups and control groups (Figure 10(B)). This result confirms the biocompatibility of NPs. As illustrated in Figure 10(C), it can be clearly observed the difference in the size of tumor among different treatment groups. This finding proves the efficacy of PHBV/PLGA NPs as a drug delivery system for treatment of cancer. The enhanced anti-tumor efficacy of 5-FU loaded in NPs may be related to passive targeting. Size of NPs is an important factor which plays a key role in the biological fate of the drug delivery system *in vivo*. According to the previous studies, particles with diameters <200 nm can readily penetrate into leaky vessels of tumor tissues based on enhanced permeability and retention (EPR) effects (Jin et al. 2011). In addition, due to low lymphatic drainage around the tumor region, NPs can accumulate selectively to the tumor tissues as compared to the free drug which is resulting in reduced side effects to others tissues (Dubey et al. 2016; Mattos et al. 2016). In the current study, size of NPs was 135 nm which make them appropriate for passive targeting by EPR effect. The present findings are in agreement with Jin et al. (2016) results which indicated that NPs with size about 100–200 nm can target tumor tissues because of EPR effect (Jin et al. 2016). Zhu et al. (2017) also suggested that nano-scaled size of doxorubicin and paclitaxel contaning NPs led to efficient passive accumulation in tumors due to EPR effect. Consequently, according to the results of previous studies and our findings, it can be concluded that effective antitumor activity of 5-FU loaded PHBV/PLGA NPs may be attributed to the EPR effect. The

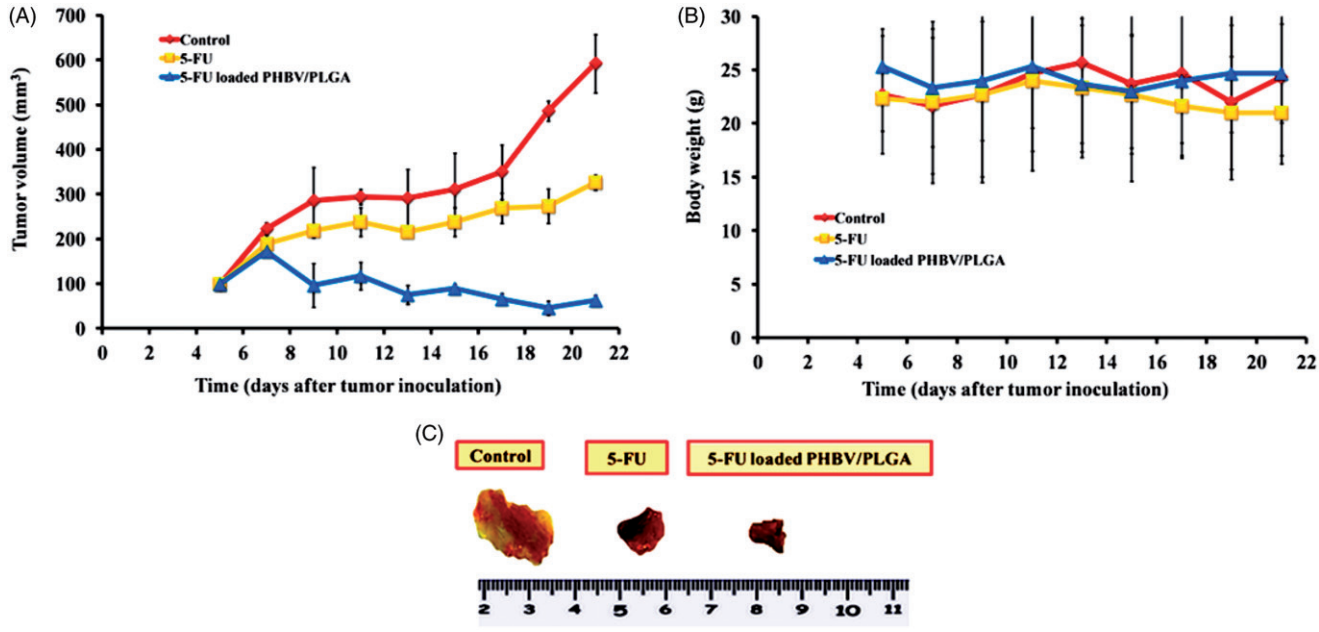

Figure 10. Evaluation of tumor growth inhibition of free 5-FU and 5-FU loaded PHBV/PLGA NPs: (A) tumor volume, (B) body weight and (C) image of solid tumor.

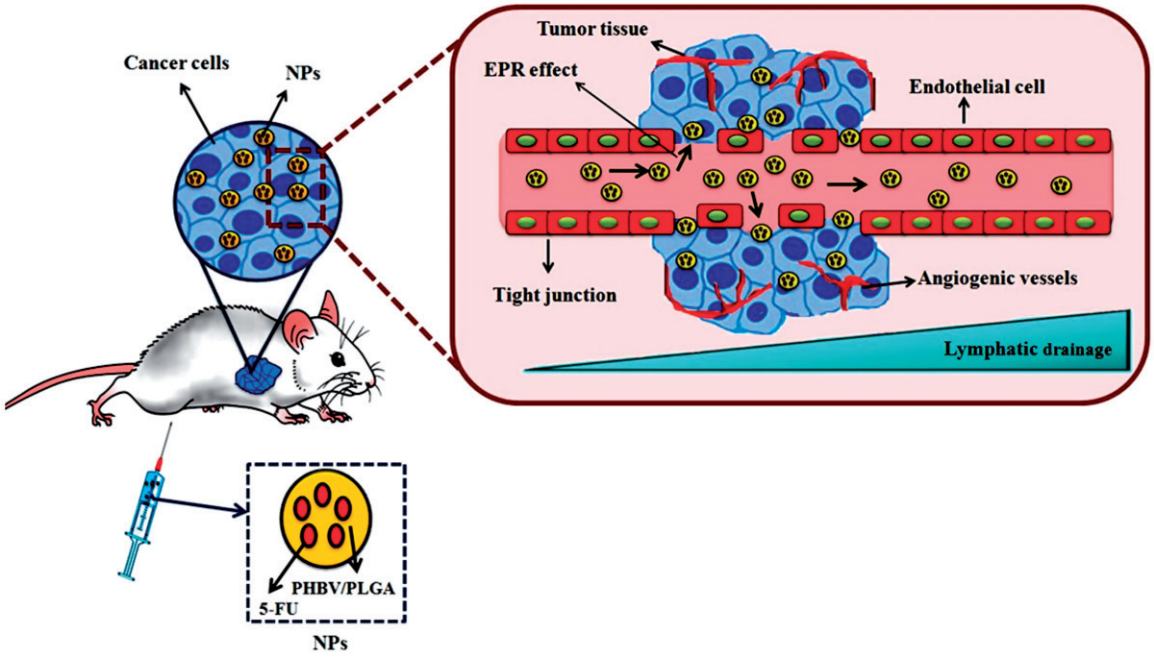

Figure 11. Schematic representation of EPR effect of PHBV/PLGA NPs in cancer cells.

proposed mechanism of EPR effect of PHBV/PLGA NPs in cancer cells is illustrated schematically in Figure 11.

4. Conclusion

In the present study, PHBV/PLGA NPs as drug delivery system for 5-FU was successfully prepared and optimized formulations were obtained using RSM. Under optimization conditions (PHBV/PLGA ratio: 3, polymers concentration: 1.7% and PVA: 2%), the EE% and particle size were 43.86% and 135 nm, respectively. NPs were spherical as demonstrated by SEM and results of DSC, TGA and FTRI also confirmed that drug successfully encapsulated into NPs. 5-FU loaded PHBV/PLGA NPs exhibited greater cytotoxicity than free drug on cancer cells. Hemolysis assay confirmed that NPs were hemo-compatible. In addition, *in vivo* anti-tumor studies revealed the higher efficacy of 5-FU loaded NPs as compared with free drug. According to the current results, it can be concluded that PHBV/PLGA NPs can be a promising delivery system for administration of drugs in cancer therapy.

Disclosure statement

The authors declare no conflict of interest.

Funding

The work was financially supported by Nanotechnology Research Center, Ahvaz Jundishapur University of Medical Sciences, Ahvaz, Iran [grant No. 111].

References

Acharya S, Sahoo SK. 2011. PLGA nanoparticles containing various anticancer agents and tumour delivery by EPR effect. Adv Drug Deliv Rev. 63:170–183.

Amin ML, Kim D, Kim S. 2016. Development of hematin conjugated PLGA nanoparticle for selective cancer targeting. Eur J Pharm Sci. 91:138–143.

Amjadi I, Rabiee M, Hosseini MS. 2013. Anticancer activity of nanoparticles based on PLGA and its co-polymer: in-vitro evaluation. Iran J Pharm Res. 12:623–634.

Chaturvedi K, Kulkarni AR, Aminabhavi TM. 2011. Blend microspheres of poly (3-hydroxybutyrate) and cellulose acetate phthalate for colon delivery of 5-fluorouracil. Ind Eng Chem Res. 50:10414–10423.

Coimbra PA, De Sousa HC, Gil MH. 2008. Preparation and characterization of flurbiprofen-loaded poly(3-hydroxybutyrate-co-3-hydroxyvalerate) microspheres. J Microencapsul. 25:170–178.

Dadashzadeh S, Derakhshandeh K, Shirazi FH. 2008. 9-Nitrocamptothecin polymeric nanoparticles: cytotoxicity and pharmacokinetic studies of lactone and total forms of drug in rats. Anticancer Drugs. 19(8):805–811.

Dobrovolskaia MA, McNeil SE. 2013. Understanding the correlation between in vitro and in vivo immunotoxicity tests for nanomedicines. J Control Release. 172:456–466.

Dubey RD, Saneja A, Qayum A, Singh A, Mahajan G, Chashoo G, Kumar A, Andotra SS, Singh SK, Singh G, Koul S, et al. 2016. PLGA nanoparticles augmented the anticancer potential of pentacyclic triterpenediol in vivo in mice. RSC Adv. 6:74586–74597.

Duran N, Alvarenga MA, Da Silva EC, Melo PS, Marcato PD. 2008. Microencapsulation of antibiotic rifampicin in poly(3-hydroxybutyrate-co-3-hydroxyvalerate). Arch Pharm Res. 31:1509–1516.

Eloy JO, Claro de Souza M, Petrilli R, Barcellos JP, Lee RJ, Marchetti JM. 2014. Liposomes as carriers of hydrophilic small molecule drugs: strategies to enhance encapsulation and delivery. Colloids Surf B Biointerfaces. 123:345–363.

Feczkó T, Tóth J, Dósa G, Gyenis J. 2011. Optimization of protein encapsulation in PLGA nanoparticles. Chem Eng Process Process Intens. 50:757–765.

Galindo-Rodriguez S, Allemann E, Fessi H, Doelker E. 2004. Physicochemical parameters associated with nanoparticle formation in the salting-out, emulsification-diffusion, and nanoprecipitation methods. Pharm Res. 21:1428–1439.

Gao H, Yang Z, Zhang S, Cao S, Shen S, Pang Z, Jiang X. 2013. Ligand modified nanoparticles increases cell uptake, alters endocytosis and elevates glioma distribution and internalization. Sci Rep. 3:2534.

Gunday Tureli N, Tureli AE, Schneider M. 2016. Optimization of ciprofloxacin complex loaded PLGA nanoparticles for pulmonary treatment of cystic fibrosis infections: Design of experiments approach. Int J Pharm. 515:343–351.

Haggar FA, Boushey RP. 2009. Colorectal cancer epidemiology: incidence, mortality, survival, and risk factors. Clin Colon Rectal Surg. 22:191–197.

Halayqa M, Domańska U. 2014. PLGA biodegradable nanoparticles containing perphenazine or chlorpromazine hydrochloride: effect of formulation and release. Int J Mol Sci. 15:23909–23923.

Huang X, Dai Y, Cai J, Zhong N, Xiao H, McClements DJ, Hu K. 2017. Resveratrol encapsulation in core-shell biopolymer nanoparticles: Impact on antioxidant and anticancer activities. Food Hydrocolloids. 64:157–165.

Huang Y, Wu C, Liu Z, Hu Y, Shi C, Yu Y, Zhao X, Liu C, Liu J, Wu Y, Wang D. 2014. Optimization on preparation conditions of Rehmannia glutinosa polysaccharide liposome and its immunological activity. Carbohydr Polym. 104:118–126.

Jain AK, Swarnakar NK, Godugu C, Singh RP, Jain S. 2011. The effect of the oral administration of polymeric nanoparticles on the efficacy and toxicity of tamoxifen. Biomaterials. 32:503–515.

Jin H, Pi J, Yang F, Jiang J, Wang X, Bai H, Shao M, Huang L, Zhu H, Yang P, et al. 2016. Folate-chitosan nanoparticles loaded with ursolic acid confer anti-breast cancer activities in vitro and in vivo. Sci Rep. 6:30782.

Jin Y, Ren X, Wang W, Ke L, Ning E, Du L, Bradshaw J. 2011. A 5-fluorouracil-loaded pH-responsive dendrimer nanocarrier for tumor targeting. Int J Pharm. 420:378–384.

Joshi G, Kumar A, Sawant K. 2014. Enhanced bioavailability and intestinal uptake of Gemcitabine HCl loaded PLGA nanoparticles after oral delivery. Eur J Pharm Sci. 60:80–89.

Khan S, Chauhan N, Yallapu MM, Ebeling MC, Balakrishna S, Ellis RT, Thompson PA, Balabathula P, Behrman SW, Zafar N, Singh MM, et al. 2015. Nanoparticle formulation of ormeloxifene for pancreatic cancer. Biomaterials. 53:731–743.

Kouhi M, Prabhakaran MP, Shamanian M, Fathi M, Morshed M, Ramakrishna S. 2015. Electrospun PHBV nanofibers containing HA and bredigite nanoparticles: Fabrication, characterization and evaluation of mechanical properties and bioactivity. Compos Sci Technol. 121:115–122.

Kudarha R, Dhas NL, Pandey A, Belgamwar VS, Ige PP. 2015. Box-Behnken study design for optimization of bicalutamide-loaded nanostructured lipid carrier: stability assessment. Pharm Dev Technol. 20:608–618.

Le VM, Wang JJ, Yuan M, Nguyen TL, Yin GF, Zheng YH, Shi WB, Lang MD, Xu LM, Liu JW. 2015. An investigation of antitumor efficiency of novel sustained and targeted 5-fluorouracil nanoparticles. Eur J Med Chem. 92:882–889.

Li W, Jan Z, Ding Y, Liu Y, Janko C, Pischetsrieder M, Alexiou C, Boccaccini AR. 2016. Facile preparation of multifunctional superparamagnetic PHBV microspheres containing SPIONs for biomedical applications. Sci Rep. 6:23140.

Lin Q, Cai Y, Yuan M, Ma L, Qiu M, Su J. 2014. Development of a 5-fluorouracil-loaded PLGA microsphere delivery system by a solid-in-oil-in-hydrophilic oil (S/O/hO) novel method for the treatment of tumors. Oncol Rep. 32:2405–2410.

Manoochehri S, Darvishi B, Kamalinia G, Amini M, Fallah M, Ostad SN, Atyabi F, Dinarvand R. 2013. Surface modification of PLGA nanoparticles via human serum albumin conjugation for controlled delivery of docetaxel. Daru. 21:58.

Masood F, Chen P, Yasin T, Fatima N, Hasan F, Hameed A. 2013. Encapsulation of ellipticine in poly-(3-hydroxybutyrate-*co*-3-hydroxyvalerate) based nanoparticles and its in vitro application. Mater Sci Eng C Mater Biol Appl. 33:1054–1060.

Matsumura Y, Maeda H. 1986. A new concept for macromolecular therapeutics in cancer chemotherapy: mechanism of tumoritropic accumulation of proteins and the antitumor agent smancs. Cancer Res. 46:6387–6392.

Mattos AC, Altmeyer C, Tominaga TT, Khalil NM, Mainardes RM. 2016. Polymeric nanoparticles for oral delivery of 5-fluorouracil:

formulation optimization, cytotoxicity assay and pre-clinical pharmacokinetics study. Eur J Pharm Sci. 84:83–91.

Mendes JB, Riekes MK, de Oliveira VM, Michel MD, Stulzer HK, Khalil NM, Zawadzki SF, Mainardes RM, Farago PV. 2012. PHBV/PCL microparticles for controlled release of resveratrol: physicochemical characterization, antioxidant potential, and effect on hemolysis of human erythrocytes. ScientificWorldJournal. 2012:1.

Nair KL, Jagadeeshan S, Nair SA, Kumar GS. 2011. Biological evaluation of 5-fluorouracil nanoparticles for cancer chemotherapy and its dependence on the carrier, PLGA. Int J Nanomed. 6: 1685–1697.

Oner M, Col AA, Pochat-Bohatier C, Bechelany M. 2016. Effect of incorporation of boron nitride nanoparticles on the oxygen barrier and thermal properties of poly(3-hydroxybutyrate-co-hydroxyvalerate). RSC Adv. 6:90973–90981.

Patel RR, Chaurasia S, Khan G, Chaubey P, Kumar N, Mishra B. 2016. Cromolyn sodium encapsulated PLGA nanoparticles: An attempt to improve intestinal permeation. Int J Biol Macromol. 83:249–258.

Patel A, Patel M, Yang X, Mitra AK. 2014. Recent advances in protein and Peptide drug delivery: a special emphasis on polymeric nanoparticles. Protein Pept Lett. 21:1102–1120.

Penaloza JP, Marquez-Miranda V, Cabana-Brunod M, Reyes-Ramirez R, Llancalahuen FM, Vilos C, Maldonado-Biermann F, Velasquez LA, Fuentes JA, Gonzalez-Nilo FD, et al. 2017. Intracellular trafficking and cellular uptake mechanism of PHBV nanoparticles for targeted delivery in epithelial cell lines. J Nanobiotechnol. 15:1.

Sadhukha T, Prabha S. 2014. Encapsulation in nanoparticles improves anti-cancer efficacy of carboplatin. AAPS PharmSciTech. 15:1029–1038.

Simion V, Stan D, Gan AM, Pirvulescu MM, Butoi E, Manduteanu I, Deleanu M, Andrei E, Durdureanu-Angheluta A, Bota M, et al. 2013. Development of curcumin-loaded poly(hydroxybutyrate-*co*-hydroxyvalerate) nanoparticles as anti-inflammatory carriers to human-activated endothelial cells. J Nanopart Res. 15:2108.

Tang Q, Wang Y, Huang R, You Q, Wang G, Chen Y, Jiang Z, Liu Z, Yu L, Muhammad S, Wang X. 2014. Preparation of anti-tumor nanoparticle and its inhibition to peritoneal dissemination of colon cancer. PLoS One. 9:e98455.

Tefas LR, Tomuta I, Achim M, Vlase L. 2015. Development and optimization of quercetin-loaded PLGA nanoparticles by experimental design. Clujul Med. 88:214–223.

Vilos C, Morales FA, Solar PA, Herrera NS, Gonzalez-Nilo FD, Aguayo DA, Mendoza HL, Comer J, Bravo ML, Gonzalez PA, Kato S, et al. 2013. Paclitaxel-PHBV nanoparticles and their toxicity to endometrial and primary ovarian cancer cells. Biomaterials. 34:4098–4108.

Xiao B, Han MK, Viennois E, Wang L, Zhang M, Si X, Merlin D. 2015. Hyaluronic acid-functionalized polymeric nanoparticles for colon cancer-targeted combination chemotherapy. Nanoscale. 7:17745–17755.

Yadav AK, Agarwal A, Rai G, Mishra P, Jain S, Mishra AK, Agrawal H, Agrawal GP. 2010. Development and characterization of hyaluronic acid decorated PLGA nanoparticles for delivery of 5-fluorouracil. Drug Deliv. 17:561–572.

Yang S, Zhang B, Gong X, Wang T, Liu Y, Zhang N. 2016. In vivo biodistribution, biocompatibility, and efficacy of sorafenib-loaded lipid-based nanosuspensions evaluated experimentally in cancer. Int J Nanomed. 11:2329–2343.

Yu Y, Lu Y, Bo R, Huang Y, Hu Y, Liu J, Wu Y, Tao Y, Wang D. 2014. The preparation of gypenosides liposomes and its effects on the peritoneal macrophages function in vitro. Int J Pharm. 460:248–254.

Zeng C, Jiang W, Tan M, Yang X, He C, Huang W, Xing J. 2016. Optimization of the process variables of tilianin-loaded composite phospholipid liposomes based on response surface-central composite design and pharmacokinetic study. Eur J Pharm Sci. 85:123–131.

Zeng X, Morgenstern R, Nyström AM. 2014. Nanoparticle-directed sub-cellular localization of doxorubicin and the sensitization breast cancer cells by circumventing GST-Mediated drug resistance. Biomaterials. 35:1227–1239.

Zhu XH, Wang CH, Tong YW. 2009. In vitro characterization of hepatocyte growth factor release from PHBV/PLGA microsphere scaffold. J Biomed Mater Res A. 89:411–423.

Zhu D, Wu S, Hu C, Chen Z, Wang H, Fan F, Qin Y, Wang C, Sun H, Leng X, et al. 2017. Folate-targeted polymersomes loaded with both paclitaxel and doxorubicin for the combination chemotherapy of hepatocellular carcinoma. Acta Biomater. 58: 399–412.